

Proposal to Measure the Cross Section of NC Inclusive π^0 Interaction Channel

Ariana Hackenburg
Yale University
ariana.hackenburg@yale.edu

July 14, 2015



Contents

1	Overview and History	4
1.1	Solar Neutrino Problem	4
1.2	Further Anomalies	5
2	Theory	6
3	LSND and MiniBooNE	6
4	Liquid Argon Time Projection Chambers (LArTPCs)	7
4.1	MicroBooNE	9
5	Current Efforts and Proposal	10
5.1	Topology	10
5.2	Reconstruction Efforts	11
5.3	Backgrounds	12
A	Appendix	14

List of Figures

1	John Bahcall's Standard Solar Flux Model	5
2	Low energy excesses seen by the LSND (left) and MiniBooNE (right) experiments	7
3	The generalized process of readout in a TPC	7
4	Readout images from the Argoneut detector. The event on the left is a signal ν_e CCQE event, while the event on the right is a background event producing a gamma	8
5	$\frac{dE}{dx}$ separation of electron vs γ [14]	9
6	Properties of MicroBooNE	9
7	MicroBooNE the model and MicroBooNE the real man. (Right) Taken when the TPC was slid into the cryostat December 2013.	10
8	Event rate prediction for 3 year run for LAr1ND and T600, 6 year run for MicroBooNE, as described in the LAr1ND January 2015 proposal to the PAC.	13
9	NC π^0 candidate found in Argoneut data	13

$$\sigma = \frac{N}{T\phi} \quad (1)$$

$$\phi = \frac{P}{AT} \quad (2)$$

ν_μ
 μ^-

$$\implies [\sigma] = L^2 \quad (3)$$

$$\sigma = Area * \frac{Number\ of\ scatters}{Number\ of\ targets * Number\ of\ incident} \quad (4)$$

$$\sigma = A * \frac{N_S}{N_T * N_I} \quad (5)$$

$$\frac{d\sigma}{dX}(X', E_T, E_S) = \frac{\frac{dN_S}{dX}(X')}{N_T * N_I} * A * \quad (6)$$

$$\nu_\mu N \rightarrow nucleons + \pi^0 + \mu \quad (7)$$

$$\nu_\mu N \rightarrow nucleons + \pi^\pm \quad (8)$$

1 Overview and History

Definitive proof for neutrino oscillation has been delivered over and over again in the last 15 years. Alongside this proof however, have come several notoriously anomalous results. In this section, we explore some of these anomalous results and their impact on the present state of neutrinos physics.

1.1 Solar Neutrino Problem

Any sort of historical review of neutrino physics at some point comes to Ray Davis, and so we might as well start our story here. In the late 1960s, Ray Davis of Brookhaven National Lab (BNL) ventured 4850ft underground in the Homestake mine with a plan to measure various contributions to solar neutrino flux [1]. Working closely with John Bahcall's theory team at CalTech, Davis' group built a tetrachloroethylene detector sensitive down to 0.814 MeV and primarily to B^8 solar neutrinos[1] a mile underground in Homestake Mine. In 1968, the group released results which revealed that a fraction of the predicted solar neutrinos were missing. This result became known as "the solar neutrino problem".

The Homestake experiment ran for 20 years, with results through the duration pointing to the same conclusion: 2/3 of the neutrinos predicted by Bahcall's Standard Solar Model (Figure 1) were not accounted for in the data[1]. Throughout the 80's and 90's, a series of experimental results from various collaborations confirmed the mysterious lack of solar neutrinos [2] [3] [9]. Kamiokande II¹, a 3 kton water Cherenkov detector built in Japan in the 80s, was only sensitive to B^8 neutrinos above 6 MeV[3] because of the surrounding radioactivity. Despite its inability to probe the keV energies of the Homestake experiment, Kamiokande II was a highly appealing detector due to its real time depiction of events and its ability to reconstruct both the energies and directions of those events[3]. Due to the unique ability of this detector, Kamiokande II was able to for the first time conclude that neutrinos were coming from the sun. In addition to this remarkable discovery, Kamiokande II also observed an apparent lack of solar neutrinos.

GALLEX was a radiochemical experiment at Gran Sasso, Italy in the 90s. GALLEX was sensitive to the pp neutrino flux energies, with a threshold of 233 keV [4]; this enabled it to probe uncharted solar flux waters. After 6 years of running, results showed solar pp flux at more than 40% that expected by the SSM². The validity of this result was confirmed with a ^{51}Cr source experiment in the detector[5]. SAGE, another Ga experiment set in Russia in the 90s observed a deficit comparable to GALLEX's. A similar test of the SAGE detector's efficiency with a ^{51}Cr source confirmed it was operating near 100% on the ^{51}Cr neutrinos[6]; these two puzzle pieces are examples of the Gallium Anomaly.

A quick recap at this point would indicate something a bit unsettling about our story thus far. The Davis experiment began digging into Bahcall's models in the 60s; yet here we were in the 90s with still no verified explanation of what was causing the observed neutrino

¹The original Kamiokande focused primarily on proton decay. After initial data taking, adjustments were made to the original detector in order to make it sensitive enough to study electron recoils from elastic neutrino scatters in water. One example addition was a surrounding layer of water which was intended to decrease background radiation. This "new" experiment was called Kamiokande II

²This only showed conclusive signs for deficit of Be^7 neutrino flux

deficit. Were neutrinos oscillating? Was something wrong with the sun[8]?

By the late 1990s, the theory of neutrino oscillation as a solution to the solar neutrino problem had been flirting with physicists for years, but remained unproven. Super Kamiokande, successor experiment to Kamiokande II, is a massive 50 kton ultra pure water detector built to investigate solar and atmospheric neutrino oscillations³. Atmospheric neutrinos originate from high energy cosmic radiation in the upper atmosphere, 15km above the surface of the earth (13000 km from the other side of the earth). The flux of atmospheric neutrinos is far smaller than that of solar neutrinos, but luckily interaction cross section increases with energy. In 1998, the Super K collaboration reported data at various energies that complied with a 2-neutrino oscillation model[7]. Quick to follow suit was the Sudbury Neutrino Observatory (SNO) in 2002. SNO was a 1 ktonne spherical deuterium Cherenkov detector located 6800ft under ground in the Creighton Mine in Sudbury[9]. The greatest barrier experiments before SNO had faced in detecting ν_μ or ν_τ interactions was that the μ and τ are heavier (105 MeV and 1777 MeV respectively) than the energy of the solar neutrino spectrum, which only extends to about 30MeV. Deuterium, which replaces the hydrogen in water with a proton and a neutron, has a dissociation energy of 2 MeV. This fact uniquely equipped SNO to measure the flux of all three neutrino flavors[9]—this total flux matched shockingly well with Bahcall’s predictions in his SSM. SNO had conclusively solved the solar neutrino problem.

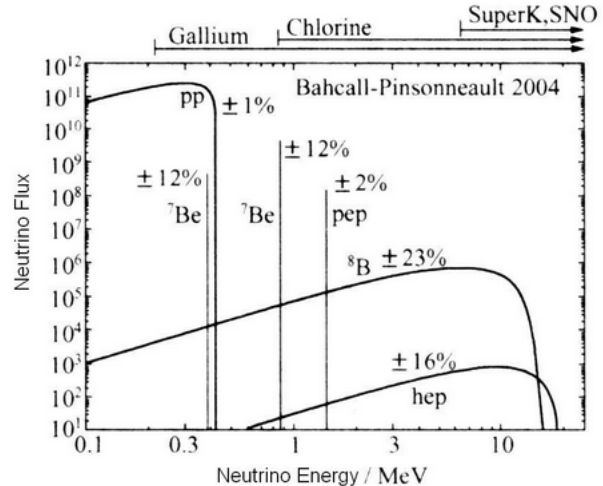


Figure 1: John Bahcall’s Standard Solar Flux Model

1.2 Further Anomalies

Double double toil and more trouble. Despite the resolution of the solar neutrino problem, further issues were brewing. As mentioned above, Super K was one of the first to tango with atmospheric neutrinos. Experiments investigating atmospheric neutrinos look primarily at directionality and zenith angle of the interactions in data. SuperK and other atmospheric neutrino experiments observed a disappearance of ν_μ , without a corresponding increase in ν_e , implying oscillation into a third neutrino, the ν_τ . As discussed above, Super K produced data which agreed with the 2 neutrino oscillation model, although they were not sensitive to the ν_τ [7]. Other experiments such as MINOS, a magnetized iron detector, produced data which matched theoretical predictions of ν_μ oscillation into ν_τ [10]. Thus rested the atmospheric neutrino anomaly.

³And primarily, to a set better limit on proton decay

2 Theory

Each neutrino flavor (ν_e, ν_μ, ν_τ) can be written as a linear combination of 3 mass eigenstates with the use of a unitary rotation matrix. It is most convenient to begin by looking at a simplified 2 neutrino oscillation model:

$$|\nu_x\rangle = \sum_{j=1,2} U_{ij} |\nu_j\rangle \quad (9)$$

Using the time-dependent Hamiltonian of the system, we can derive a probability of oscillation from flavor α to flavor β (see Appendix A for more detail about this derivation). After propagating these states in time and doing some rearranging, we arrive at

$$P(\nu_\alpha \rightarrow \nu_\beta) = \sin^2(2\theta) \sin^2(1.27 \Delta m^2 \frac{L}{E}) \quad (10)$$

where θ is the mixing angle of the oscillation, Δm^2 is the frequency of neutrino oscillation, L is the length the neutrino traveled and E is the energy of the neutrino at its source. It is clear then that $\frac{L}{E}$ is the experimentally controllable parameter—an experiment's choice of $\frac{L}{E}$ depends on the ranges Δm^2 and $\sin^2(2\theta)$ it wishes to probe.

It is useful to look at an example of how the free parameter affects sensitivity. An experiment is most sensitive to Δm^2 for $\Delta m^2 \approx E/L$. In addition, the neutrino beam diverges $\propto \frac{1}{L^2}$. So an experiment with a short baseline (small L) has the benefit of seeing lots of events (ie, has high sensitivity to $\sin^2(2\theta)$), and is sensitive only to large values of Δm^2 [11].

3 LSND and MiniBooNE

In the last 20 years, a variety of other experimental results have indicated that the 3-neutrino oscillation model (and thus, the Standard Model), may not be complete. Liquid Scintillator Neutrino Detector (LSND), a scintillation detector in a stopped pion beam from the 90's, expected the majority of its events to come from ν_μ and $\bar{\nu}_\mu$, with a small fraction of $\bar{\nu}_e$ interactions—in their results, they observed an excess of low energy electron anti-neutrino events for $\frac{L}{E} \sim 1 \frac{m}{MeV}$ (Figure 2), explained at the time with a simple 2-neutrino oscillation model [13]. These unexpected results led to the construction of the Mini Booster Neutrino Experiment (MiniBooNE), a Cherenkov detector in Booster Neutrino Beam (BNB) at Fermilab. After 10 years of running, MiniBooNE's data revealed an excess of low energy events in both neutrino and anti-neutrino modes at energies below and incorporating LSND's data (Figure 2) ⁴. These results did a couple important things: first, MiniBooNE's data refuted the previous 2-neutrino oscillation explanation [12], and second, it called into question the nature of the observed low-energy excess. In a Cherenkov detector, electromagnetic showers such as the electron and single photon both have a fuzzy-ring signature (as opposed to a muon, which leaves a distinct ring signature). This makes it impossible to distinguish an

⁴MiniBooNE also observed different amounts of excess in neutrino and anti-neutrino mode, leading to additional questions about nuclear interactions, cross sections and the relationship between the neutrino and antineutrino[12]

electron neutrino event from a photon produced in a background reaction. So MiniBooNE which had set out to resolve an anomaly left one of its own: what was causing this low energy excess?

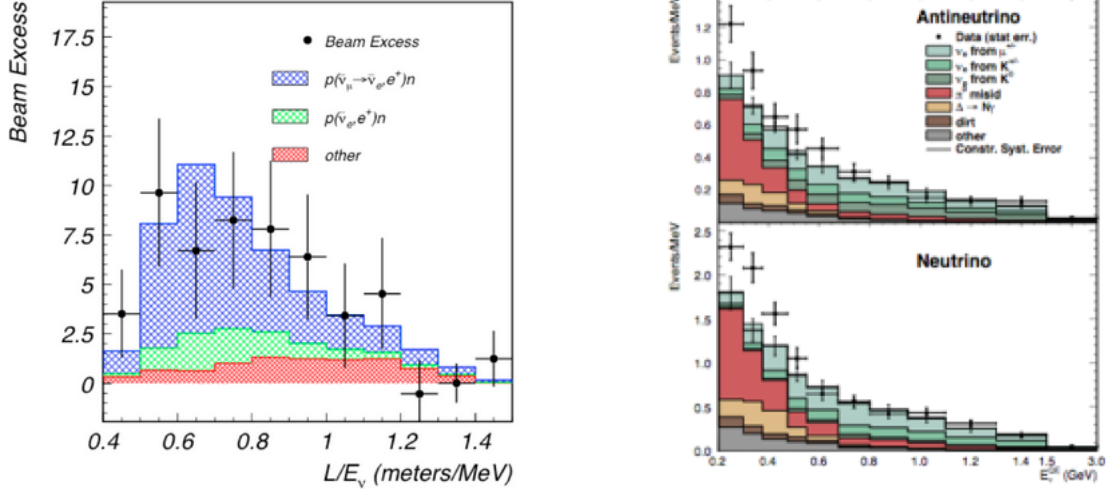


Figure 2: Low energy excesses seen by the LSND (left) and MiniBooNE (right) experiments

4 Liquid Argon Time Projection Chambers (LArTPCs)

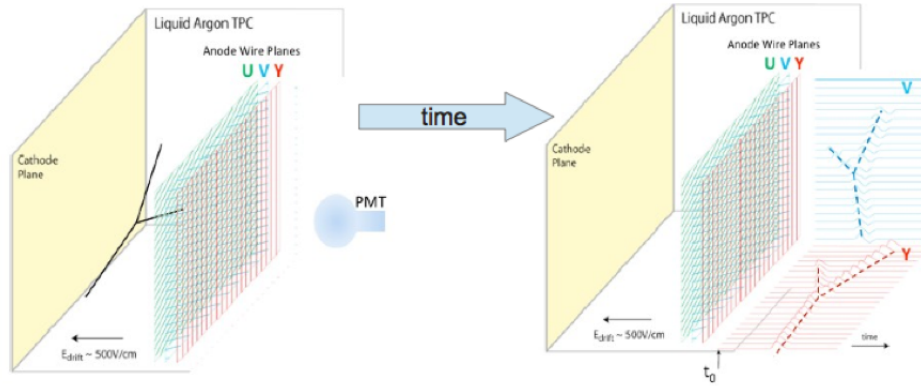


Figure 3: The generalized process of readout in a TPC

Liquid Argon Time Projection Chambers (LArTPCs) are ideal detectors for neutrino oscillation experiments with short and long baselines. There are a number of properties that make Liquid Argon (LAr) well suited for the TPC medium: it is cheap, easy to cool, and transparent to its own scintillation light. When a charged particle travels through a TPC in LAr, it leaves a trail of ionization electrons (and excited LAr dimers) that are drifted in a uniform electric field to wire readout planes.

Readout from the wires makes the Y and Z coordinates of an interaction accessible, while the drift time acts as the third X coordinate; scintillation signals seen by an array of PMTs also play an important role in making the drift direction accessible⁵. Thus a LArTPC with 3 (or 2) planes gives us the capability to reconstruct fine-grained, 3 dimensional configurations of events in the detector.

Two of the primary benefits of using a TPC as your detector is that you get calorimetric information + image quality resolution as seen in Figure 4. These event displays depict example events in which an electron, gamma were produced respectively. At first glance, a somewhat obvious distinction between the two events is the gap between the start of the shower and vertex in the display on the right. This gap is associated with a gamma and is due to our inability to detect neutral particles directly. In other words, we do not see the gamma until it pair produces or Compton scatters in the detector, at which point we observe an electro-magnetic (EM) shower. In contrast to the birth of the gamma EM shower, the electron EM shower is seen as soon as the electron is born⁶. When an electron scatters off an Argon atom, it produces a Bremsstrahlung photon which then pair produces, etc leading to an EM shower with no gap. This topological cut is a powerful tool in discriminating between the interactions that caused grief for MiniBooNE.

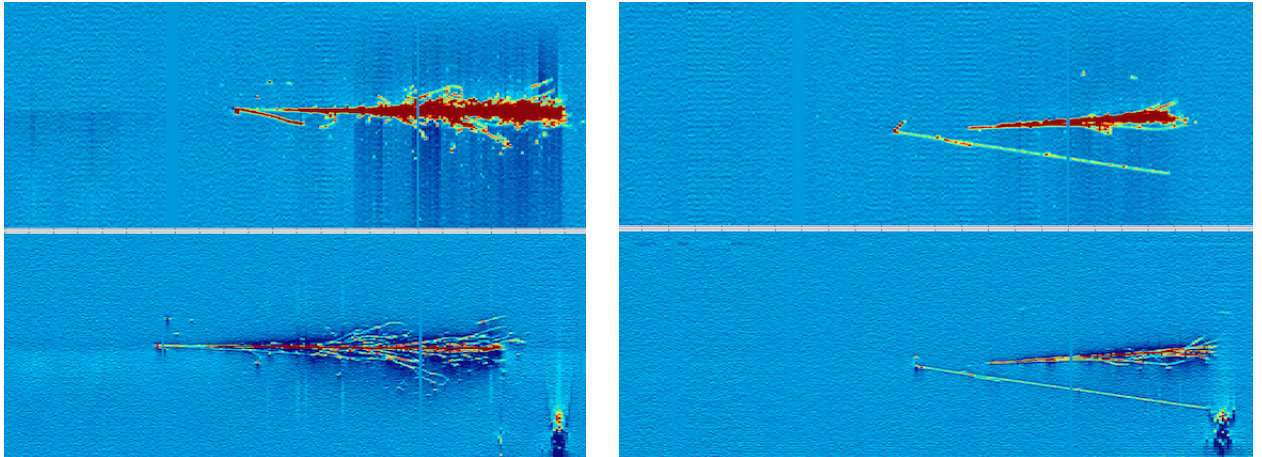


Figure 4: Readout images from the Argoneut detector. The event on the left is a signal ν_e CCQE event, while the event on the right is a background event producing a gamma

There is one caveat to the story thus far, but it has a pleasant solution so fear not! Monte Carlo simulations show us that the photon can sometimes pair produce near enough to the vertex of interaction to appear gap-less. In addition, the signature of a neutral current (NC) ν_e event is a single shower with no vertex activity. This casts doubt (or at least a decrease in event selection efficiency) on the signal sample selected by just the topology cut. But there is something we have not used yet. An electron is a minimally ionizing particle (MIP) leaving $\sim 2 \frac{\text{Mev}}{\text{cm}}$ behind in its wake. When a gamma pair produces (accounts for $\sim 94\%$ of events

⁵It is important to note that the success of a LArTPC does not rely on PMTs to extract "X"—this extra piece of information establishes t_0 in correspondance with the beam gate, while also tagging backgrounds events which occur in the beam window.

⁶That is, assuming it is above some threshold.

above 150 MeV), it creates 2 MIPs. Thus if we examine the first few cm ($\sim 2.4\text{cm}$) of the shower, we should see an energy deposition per cm ($\frac{dE}{dx}$) of 1 MIP for an electron shower and 2 MIPs for a gamma shower [14]. This technique allows us to distinguish between gammas and electrons with high efficiency. A successful example of this discrimination technique is shown for Argoneut data below in Figure 5.

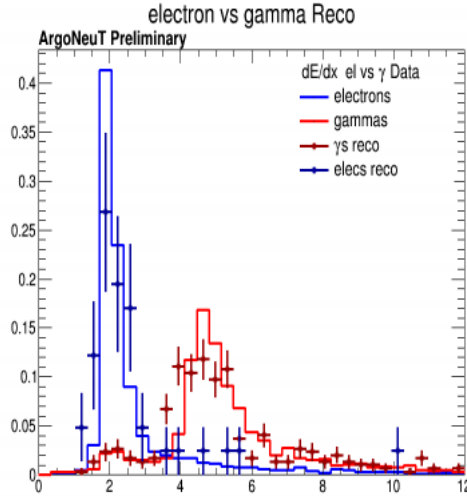


Figure 5: $\frac{dE}{dx}$ separation of electron vs γ [14]

4.1 MicroBooNE

MicroBooNE, the latest in a series of Booster Beam experiments located at Fermilab, is a Liquid Argon Time Projection Chamber (LArTPC) that will investigate the low energy neutrino excess seen by its predecessor, MiniBooNE. Cherenkov detectors, such as MiniBooNE, are limited by their inability to distinguish between single electrons and photons, a task LArTPCs are well suited for, as described in more depth above. With the high precision reconstruction capabilities of a LArTPC, MicroBooNE will be able to determine with high statistical certainty whether electrons or photons caused the anomalous MiniBooNE low energy excess. Of further interest to MicroBooNE, and the further proposal of this prospectus, are various neutrino-nucleon interaction cross-sections. Cross sections have accounted for much of the uncertainty in recent results from a variety of neutrino experiments[12] and sensitive measurements by MicroBooNE have the potential to lead to improved nuclear models and rate predictions. Beyond MicroBooNE, LArTPCs will continue to play a notable role in oscillation physics. LAr1-ND will act as a baseline for improving systematic uncertainties in MicroBooNE and investigating the nature of the MiniBooNE excess, while also acting as a

MicroBooNE Detector	
Medium	Liquid Argon
Temperature	87.3 K
Electric Field	500 V/cm
Drift Velocity	1.63 mm/ μ s
Drift Time	1.63 ms
Light Collection	32 8" PMTs 4 light guide prototypes
Readout	8256 wires 3 planes 3 mm pitch

Figure 6: Properties of MicroBooNE

small-scale phase experiment for future, bigger LArTPCs such as and LBNF. MicroBooNE is currently getting ready to commission the detector.

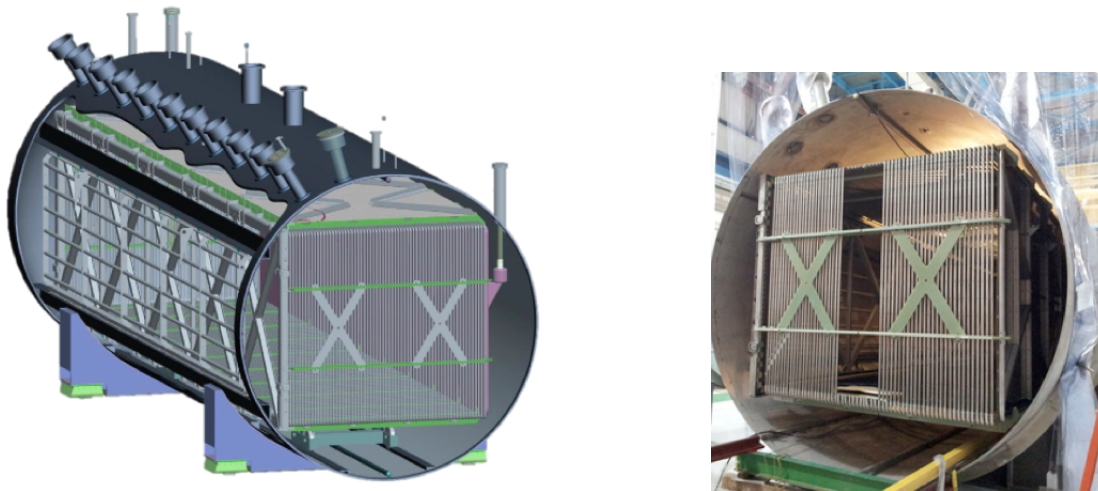


Figure 7: MicroBooNE the model and MicroBooNE the real man. (Right) Taken when the TPC was slid into the cryostat December 2013.

5 Current Efforts and Proposal

The proposal of this prospectus is to measure an inclusive neutral current (NC) π^0 interaction cross section. In this case, we take "inclusive" to indicate all interactions which conclude with a single π^0 and no other mesons. This condition purposefully includes all final state interactions (FSI) in order to decrease model dependent uncertainties, and limit this study to production we can feasibly see in the detector. The elimination of a state-dependent model also makes the cross section measurement itself more useful for the experiment. π^0 events act as one of MicroBooNE's primary background candidates; because MicroBooNE's flagship analysis will be a ν_e appearance search, it is crucial to have a well-characterized background (naturally categorized under this banner of inclusiveness). Thus, our first goal is to identify what will constitute the signal of this study, a NC π^0 .

5.1 Topology

A neutral current interaction is one in which a Z^0 is exchanged between the neutrino in initial and final states. This is in contrast with a charged current (CC) interaction where a charged W boson is exchanged between the incoming neutrino and outgoing charged lepton. Thus, one of the things we can expect NOT to see when we search for NC π^0 events is a charged lepton leaving a production vertex; this gives us good discriminatory power against CC events. The topology of the π^0 itself is also very distinct. When a π^0 is produced, it quickly decays into 2 γ 's (and very rarely, into 3). The π^0 signature we'll look for is thus 2 EM showers separated from a vertex defined either by hadronic activity or by nothing, but no other charged leptons or mesons.

It is worth noting that there are several ways a π^0 can be mistaken for signal ν_e :

- 1) One shower is not contained, in which case the π^0 will appear to be a single EM shower.
- 2) One shower is absorbed by/lost in the detector.
- 3) The showers have a small angle with respect to one another and appear to be one shower in readout.

These pieces of information will be taken into account when calculating the efficiency of this analysis.

5.2 Reconstruction Efforts

One of the most important tasks on this side of data taking is to ensure that reconstruction is in a ready-to-go state when data becomes available. Automating reconstruction is crucial for the new generation of LArTPCs which will rack in more than a million neutrino events per year, and of course also to perform an efficient analysis in MicroBooNE. Track reconstruction has existed for some time now, dating back to the days of Argoneut; shower reconstruction, on the other hand, has not. This major undertaking was begun around a year ago and takes place in several stages. Crudely, hits are joined into clusters by plane (merged) and then joined across the planes (matched) using a variety of algorithms. Once the shower clusters have been matched across planes, the shower goes through "3D reconstruction" and becomes a usable shower object with energy, momenta, angle, charge profile, start and end points, etc. We combine this shower and track information on a per event basis to create an additional vertex object, representative of the interaction location. These three objects in conjunction with variables such as $\frac{dE}{dx}$, radiation length, etc, allow us to assign log likelihood to event topologies per event category. Currently, (after background removal), the likelihood that an event contains a π^0 depends on several things:

- 1) There are at least 2 showers in the event
- 2) Each shower should be more likely a gamma than an electron
- 3) The showers must project back to the same vertex
- 4) The calculated invariant mass must be close to the expected $135.0 \frac{MeV}{c^2}$ (Equation 11)

$$M_{\pi^0}^2 = 4E_{\gamma_1}E_{\gamma_2}\sin^2\frac{\theta}{2} \quad (11)$$

Once an event is tagged as "likely to be" a π^0 , there are two important quantities which must be kept in mind. Sample selection effectiveness (or efficiency) is the number of events remaining after cuts. Purity is the percentage of the signal sample remaining after cuts. An important thing to keep in mind is that purity must be measured according to reconstructed kinematics.

Ultimately, these reconstruction efforts will lead to a series of interaction channel cross section measurements. To do a cross section measurement, there are several pieces of information that we need to obtain. The cross section is given by Equation 12 below:

$$N_{obs} = \sigma * \Phi * \epsilon \quad (12)$$

where N_{obs} is number of interactions selected from the reconstruction described above, Φ is the flux of the interaction of interest and ϵ is the efficiency with which events are selected. The flux of the BNB has been well characterized by the MiniBooNE collaboration [12]. If our reconstruction were perfect, and our sample efficiency and purity were both 1, then we would divide our event rate by total flux and we would be done. But our samples will not be pure, nor will they be selected with 100% efficiency—background events will inevitably leak in, and we lose signal to our series of cuts. Detector effects may also lead to "smearing" of kinematic variables which must be in some sense "unsmeared" before we work with them. This means the real lifting comes in estimating our efficiency, and correcting for it. There are a few aspects of estimating efficiency of event selection. The first is that efficiency is energy dependent. One way to overlook this issue is to calculate a differential cross section of our channel of interest on Ar with respect to energy. Another issue is that estimating the efficiency of our automated reconstruction is tricky. With a limited sample of un-blinded data, we won't have high statistics and will possibly need to rely on MC truth estimates to produce this number.

It is worth noting only 3 such π_0 cross section measurements from K2K, SciBooNE and MiniBooNE to this day [17][18][15].

5.3 Backgrounds

MicroBooNE, a surface dweller, is subject to constant bombardment by cosmic radiation from the upper atmosphere. Gammas from these upper atmosphere cascades can Compton scatter or pair produce in the detector, resulting in either an electron shower from the former, or electron/positron showers from the latter. These backgrounds have the potential to mimic MicroBooNE's primary signal, a single electron shower, and to muddy our π_0 sample. To filter these background events from data, various parameters of interactions were examined. For instance, most gamma radiation comes from above the detector; it is thus reasonable to expect many cosmic showers to have a downward trajectory. As another example, the interaction length in Liquid Argon (14cm) limits the distance we can expect a Compton gamma to travel before interacting. At the end of 2014, major efforts were undertaken to estimate these cosmogenic backgrounds [16].

The strategy of this study was the following: using a Monte Carlo sample, examine both cosmic events which can be correlated to charged tracks and those which cannot be. While Compton scatters are much lower energy, and thus mostly eliminated by the energy cuts we invoke for signal events, the ones that sneak through are dangerous. They mimic ν_e signal with little apparent discrimination. The pair producing photons, while higher energy and most likely to mimic our π_0 signal, are mostly eliminated by the $\frac{dE}{dx}$ cut described above.

While this study was primarily targeted towards estimating a cosmogenic background for signal ν_e events, it can be extended to estimate a π_0 background as well. Other studies for dirt background (neutrino interactions in material external to the detector whose byproducts end up in the detector) are also being undertaken.

On a final note, we can potentially extend the depths of the study described above

	LAr1-ND 6.6×10^{20} p.o.t.	MicroBooNE 13.2×10^{20} p.o.t.	ICARUS-T600 6.6×10^{20} p.o.t.
$\mu \rightarrow \nu_e$	6,712	338	607
$K^+ \rightarrow \nu_e$	7,333	396	706
$K^0 \rightarrow \nu_e$	1,786	94	180
NC $\pi^0 \rightarrow \gamma\gamma$	1,356	81	149
NC $\Delta \rightarrow \gamma$	87	5	9
ν_μ CC	484	35	51
Dirt events	44	47	67
Cosmogenic events ^a	170 (9)	220 (11)	204 (10)
Signal ($\Delta m^2 = 0.43 \text{ eV}^2$, $\sin^2 2\theta = 0.013$) [34]	114	136	498

Figure 8: Event rate prediction for 3 year run for LAr1ND and T600, 6 year run for MicroBooNE, as described in the LAr1ND January 2015 proposal to the PAC.

to investigate in more depth the underlying physics of exclusive channel production of π^0 . The exclusive channels of neutral current π^0 production are the coherent and incoherent channels. In coherent π^0 production, the neutrino interacts with the whole nucleus to produce a π^0 (Equation 13). In constrast, a neutrino with a bit more momentum can interact with a nucleon or constituent quark (Equation 14) and cause incoherent π^0 production. The latter interactions occur more prevalently at higher momentum transfers, and have the potential to produce very messy event displays (particularly in the case of quark excitation). A measurement such as this also requires us to invoke an FSI model, particularly for an incoherent measurement; for every π^0 we see, we need to account for those which were absorbed or exchanged in the nucleus, and thus not seen in the detector.

$$\nu_\mu A \rightarrow \nu_\mu \pi^0 A \quad (13)$$

$$\nu_\mu N \rightarrow \nu_\mu \pi^0 N \quad (14)$$

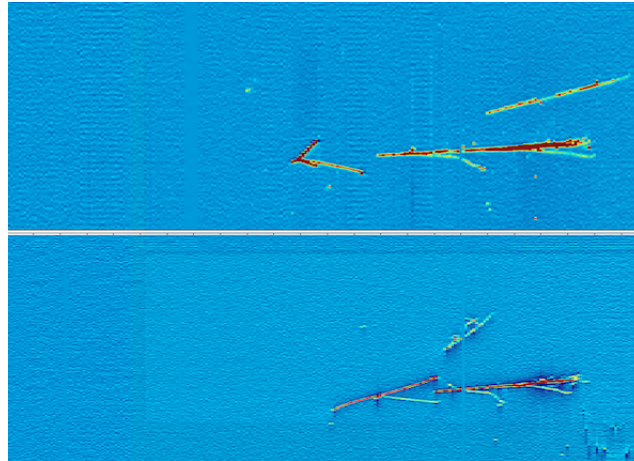


Figure 9: NC π^0 candidate found in Argoneut data

A Appendix

In the 2 neutrino oscillation model, we represent a flavor state as the linear combination of mass eigenstates via a unitary matrix

$$|\nu_x\rangle = \sum_{j=1,2} U_{ij} |\nu_j\rangle \quad (15)$$

A 2 dimensional unitary rotation matrix can be written as

$$U = \begin{bmatrix} \cos(\theta) & \sin(\theta) \\ -\sin(\theta) & \cos(\theta) \end{bmatrix} \quad (16)$$

Using this unitary matrix, we can re-write equation 15

$$\begin{bmatrix} \nu_\alpha \\ \nu_\beta \end{bmatrix} = \begin{bmatrix} \cos(\theta) & \sin(\theta) \\ -\sin(\theta) & \cos(\theta) \end{bmatrix} \begin{bmatrix} \nu_1 \\ \nu_2 \end{bmatrix} \quad (17)$$

In order to put equation 17 into a more meaningful form, it is useful to put both sides into flavor basis. To start this process, we recall that we can use the time propagator to represent evolution in time. For simplicity, we also re-write the $Et - \vec{p} \cdot \vec{x}$

$$\begin{bmatrix} \nu_1(t) \\ \nu_2(t) \end{bmatrix} = \begin{bmatrix} e^{-i\phi_1} & 0 \\ 0 & e^{-i\phi_2} \end{bmatrix} \begin{bmatrix} \nu_1(0) \\ \nu_2(0) \end{bmatrix} \quad (18)$$

Then, using the inverse of equation 17, we can rewrite

$$\begin{bmatrix} \nu_1(0) \\ \nu_2(0) \end{bmatrix} = \begin{bmatrix} \cos(\theta) & -\sin(\theta) \\ \sin(\theta) & \cos(\theta) \end{bmatrix} \begin{bmatrix} \nu_\alpha(0) \\ \nu_\beta(0) \end{bmatrix} \quad (19)$$

Combining equations 17, 19, we can represent time propagated flavor basis as

$$\begin{bmatrix} \nu_\alpha(t) \\ \nu_\beta(t) \end{bmatrix} = \begin{bmatrix} \cos(\theta) & \sin(\theta) \\ -\sin(\theta) & \cos(\theta) \end{bmatrix} \begin{bmatrix} e^{-i\phi_1} & 0 \\ 0 & e^{-i\phi_2} \end{bmatrix} \begin{bmatrix} \cos(\theta) & -\sin(\theta) \\ \sin(\theta) & \cos(\theta) \end{bmatrix} \begin{bmatrix} \nu_\alpha(0) \\ \nu_\beta(0) \end{bmatrix} \quad (20)$$

Instead of simplifying this any further, we look at a test case. Assume a beam is produced in a pure ν_β state at $t=0$. To find the probability that at time t a ν_β in the beam has oscillated into a ν_α , we calculate the square of the probability amplitude:

$$\begin{aligned} | \langle \nu_\beta(0) | \nu_\alpha(t) \rangle |^2 &= | \langle \nu_\beta(0) | \cos\theta \sin\theta (e^{-i\phi_1} - e^{-i\phi_2}) | \nu_\beta(0) \rangle |^2 \\ &= (\cos\theta \sin\theta)^2 (1 + 1 + e^{i(\phi_1 - \phi_2)} + e^{-i(\phi_2 - \phi_1)}) \\ &= 2(\cos\theta \sin\theta)^2 (1 - \cos(\phi_1 - \phi_2)) \\ &= \sin^2 2\theta \sin^2\left(\frac{\phi_1 - \phi_2}{2}\right) \end{aligned} \quad (21)$$

At this point, our probability formula is almost in its familiar form. To finalize, we recall from above that the phase shift ϕ is $E_i t - p_i x$ and make the following assumptions:

- 1) At $v \sim c$, $x \sim t \sim L$

2) Mass eigen states are created with equal energy Now ϕ_i can be written

$$\begin{aligned}\phi_i &= (E - p_i)L \\ \text{where } p_i &\approx E(1 - \frac{1}{2} \frac{m_i^2}{E}) \\ \implies \phi_2 - \phi_1 &= \frac{1}{2} \frac{L}{E} (\Delta m_2^2 - \Delta m_1^2)\end{aligned}\tag{22}$$

which leads us to the probability of oscillation from ν_β to ν_α :

$$P(\nu_\beta \rightarrow \nu_\alpha) = \sin^2(2\theta) \sin\left(\frac{1}{4} \frac{L}{E} \Delta m_{12}^2\right)\tag{23}$$

References

- [1] Davis, Raymond, and Don S. Harmer. "Solar Neutrinos." *Solar Neutrinos*. (1964): n. page. Print.
- [2] Cleveland, Bruce T., et al. "Measurement of the Solar Electron Neutrino Flux with the Homestake Chlorine Detector." *ApJ*. 496.505 (1998): n. page. Print.
- [3] Hirata, K. S., et al. "Real-time, directional measurement of 8 solar neutrinos in the Kamiokande II detector." *Phys. Rev. D*. 44.2241 (1991): n. page. Print.
- [4] Hampel, W., et al. "GALLEX solar neutrino observations: Results for GALLEX IV." *Phys. Lett. B*. 447. (1999): 127-133. Print.
- [5] Hampel, W., et al. "Final results of the ^{51}Cr neutrino source experiments in GALLEX." *Phys. Lett.*. 420.1-2 (1998): 114-126. Print.
- [6] Abdurashitov, J. N., et al. "The Russian-American Gallium Experiment (SAGE) Cr Neutrino Source Measurement." *Phys. Rev. Lett.* (1996): n. page. Print.
- [7] Fukuda, Y., et al. "Evidence for Oscillation of Atmospheric Neutrinos." *Phys. Rev. Lett.*. (1998): n. page. Print.
- [8] Clarke, Arthur C. *The Songs of Distant Earth*. Del Rey Books, 1986. Print.
- [9] McGregor, Gordon A. "FIRST RESULTS FROM THE SUDBURY NEUTRINO OBSERVATORY." *arXiv*. (2002): n. page. Print.
- [10] Adamson, P., et al. "Measurement of Neutrino and Antineutrino Oscillations Using Beam and Atmospheric Data in MINOS." *Phys. Rev. Lett.*. 110.251801 (2013): n. page. Print.
- [11] Boyd, Steve. "Neutrino Oscillations." *PX435 Neutrino Physics*. N.p.. Web. 19 Feb 2015. http://www2.warwick.ac.uk/fac/sci/physics/current/teach/modulei_home/px435/lec_oscillations.pdf.
- [12] MiniBooNE Collaboration. "The Neutrino Flux prediction at MiniBooNE." *Phys. Rev. D*. (2008): n. page. Print.
- [13] Aguilar, A., et al. "Evidence for Neutrino Oscillations from the Observation of Electron Anti-neutrinos in a Muon Anti-Neutrino Beam." *Phys. Rev. D*. (2001): n. page. Print.
- [14] Szlec, A. M. "Recent Results from ArgoNeuT and Status of MicroBooNE." *Proceedings from Neutrino 2014*. (2014): n. page. Print.
- [15] Anderson, Colin. "Measurement of Muon Neutrino and AntiNeutrino Induced Single Neutral Pion Production Cross Section." *Thesis*. (2011): n. page. Print.
- [16] Caratelli, D., et al. "Electron Neutrino Cosmogenic Background Mitigation in MicroBooNE." *Technote 3978*. (2014): n. page. Print. http://www-microboone.fnal.gov/at_work/technotes.html.

-
- [17] Nakayama, S., et al. "Measurement of single π^0 production in neutral current neutrino interactions with water by a 1.3 GeV wide band muon neutrino beam." *Phys. Lett. B.* 619.255-262 (2004): n. page. Print.
- [18] Kurimoto, Y., et al "Measurement of inclusive neutral current π^0 production on carbon in a few-GeV neutrino beam." *Phys. Rev. D.* 81. (2010): n. page. Print.